Article:
Conteduca, D., Dell'Olio, F., Ciminelli, C. et al. (2 more authors) (2016) Design of a high-performance optical tweezer for nanoparticle trapping. Applied Physics A. 295. pp. 1-6. ISSN 1432-0630

https://doi.org/10.1007/s00339-016-9894-0

Design of a high performance optical tweezer for nanoparticle trapping

D. Conteduca[1], F. Dell'Olio[1], C. Ciminelli[1], T. F. Krauss[2], M. N. Armenise[1]
[1] Optoelectronics Laboratory, Politecnico di Bari, Via E. Orabona, 4, 70125 Bari, Italy.
[2] Photonics Group, Department of Physics, University of York, Heslington, YO10 5DD, York, UK.
Tel: +39 080 596 3492, Fax: +39 080 596 3410, e-mail: caterina.ciminelli@poliba.it

Abstract

Integrated optical nanotweezers offer a novel paradigm for optical trapping, as their ability to confine light at the nanoscale leads to extremely high gradient forces. To date, nanotweezers have been realised either as photonic crystal or as plasmonic nanocavities. Here, we propose a nanotweezer device based on a hybrid photonic/plasmonic cavity with the goal of achieving a very high Quality factor over mode volume (Q/V) ratio. The structure includes a 1D photonic crystal (PhC) dielectric cavity vertically coupled to a bowtie nanoantenna. A very-high Q/V ~ 10^7 $(\lambda/n)^{-3}$ with a resonance transmission T = 29% at λ_R = 1381.1 nm has been calculated by 3D Finite Element Method (FEM), affording strong light-matter interaction and making the hybrid cavity suitable for optical trapping. A maximum optical force F = -4.4 pN, high values of stability S = 30 and optical stiffness k = 90 pN/nm·W have been obtained with an input power P_{in} = 1 mW, for a polystyrene nanoparticle with a diameter of 40 nm. This performance confirms the high efficiency of the optical nanotweezer and its potential for trapping living matter at the nanoscale, such as viruses, proteins or small bacteria.

Keywords: Photonic cavity, Photonic crystals, Plasmonics, Optical trapping, Nanotweezer.

1. Introduction

In recent years, optical techniques have been developed to trap small cells and bacteria; using light forces instead of mechanical forces prevents direct contact with the target object, as required by several medical applications for which non-invasive and non-destructive testing is necessary in order to prevent damage or disruption [1]. In order to improve the interaction, resonant cavities can be used, such as PhC cavities and microring configurations, which allow a stronger confinement of the optical energy and offer a stronger gradient force than the Gaussian beams conventionally used [2-5]; in fact, resonant cavity trapping already enables nanoscale manipulation of small viruses and proteins with sizes smaller than 100 nm [4]. Regarding the type of cavity to be used, microring resonators typically allow weaker light-matter interaction in comparison with PhC cavities. Nevertheless, stable trapping of polystyrene particles with a diameter of 500 nm has been demonstrated with microring resonators in SOI technology [6] and stable trapping of 200 nm particles has also been shown with microdonut configurations [7].
A stronger energy confinement, which corresponds to a lower mode volume combined with a high Q-factor, is typically obtained by PhC configurations. For example, small nanoparticles with a diameter of 100 nm or less have already been trapped with PhC cavities [7] and a single bacterium of *Escherichia Coli* with a cross-section of 1μm^2 has been trapped for a long time (> 5 min) using only low input power (P_{in} < 1 mW) [8]. Going further down in lengthscale, an optical nanotweezer with a 1D PhC cavity able to trap a single protein as small as 22 nm has been proposed in [9]. If realised experimentally, such performance levels make these nanocavities suitable for a number of life science applications, e.g. in biology, oncology and proteomics [10]. However, dielectric microcavities are diffraction limited, so their mode volume can only be decreased so far. Plasmonic cavities do not suffer this limitation because surface plasmon polariton (SPP) modes are strongly confined at the metal-dielectric interface, so strongly enhancing the trapping force [11]. Their very low mode volume V < 10^{-4} $(\lambda/n)^3$ operation enables a strong interaction between light and the target object [12] and has already been used to demonstrate the trapping of metal nanoparticles with a diameter smaller than 10 nm [13,14] and of a single bovine serum albumin (BSA) molecule with a size of 3 nm [15]. The issue with plasmonic cavities, however, is that the metallic losses cause thermal heating, which makes the traps unstable and increases the risk of damage to living matter at the nanoscale as well as increasing the risk of damage to living matter [17].
As an alternative, hybrid dielectric/plasmonic cavities represent a better tradeoff between spectral and spatial energy densities and low optical losses [18]. Several configurations of hybrid cavities have already been proposed. These cavities obtain values of the mode volume comparable with those obtained by plasmonic structures (V ~ 10^{-4} $(\lambda/n)^3$), but have lower optical losses and higher Q-factors (Q ~ 10^2), which corresponds to Q/V ~ $10^5(\lambda/n)^{-3}$ [19]. A remarkable advantage of hybrid configurations is that they enable strong energy confinement in the medium with lower refractive index, unlike dielectric cavities, which makes them very suitable for biosensing applications and optical trapping due to the resulting strong light-matter interactions [2]. As a result, the trapping of proteins with a diameter smaller than 10 nm has already been verified [20] in a hybrid cavity.
Here, we propose a photonic/plasmonic device, based on the vertical coupling between an 1D PhC cavity and a bowtie nanoantenna, that provides an even higher Q/V ratio (~10^7 $(\lambda/n)^{-3}$) combined with a good detection resolution due to the resonance transmission T = 29%. Note that typical plasmonic cavities only achieve a resonant transmission of order of a few percent, so this high value of transmission is a major improvement. We also observe strong energy confinement at the tips of

the nanoantenna, thus strongly increasing light-matter interaction. These hotspots provide high optical forces in the pN-range with low input power ($P \leq 1$mW) around the nanoantenna. We also show that the hybrid cavity features high stability, defined as the ratio between trapping energy and thermal energy, which makes it suitable as an optical nanotweezer for trapping, especially of living matter at the nanoscale.

2. Device configuration

The hybrid cavity is based on a 1D photonic crystal dielectric cavity in silicon-on-insulator (SOI) technology vertically coupled to a plasmonic nanoantenna in Au, as shown in Fig. 1. The PhC is realized in a silicon nanowire, positioned on a SiO_2 layer with a thickness of 2 μm. The dielectric cavity has two mirror sections, each one containing four holes with a fixed radius R and a period Λ, and two symmetric tapering sections containing six holes with different radii R_i and periods Λ_i. The holes' radii R_i and periods Λ_i gradually increase from the middle of the cavity to the mirror section in order to match the cavity mode to the Bloch mode of the mirror [21].

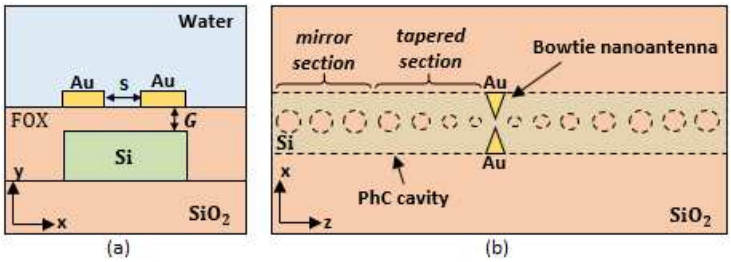

Fig.1 (a) Cross-section and (b) top view of the photonic/plasmonic cavity.

The plasmonic nanoantenna is placed above the PhC dielectric cavity to funnel the light vertically on resonance. There is a strong refractive index contrast at the interfaces between Au and dielectric materials, so in order to respect the continuity of the normal component of the electric flux density D ($\hat{n}\cdot(D_{met} - D_{diel}) = 0$), strong light confinement is typically observed in the material with the lower relative permittivity, which here corresponds to the water surrounding the nanoantenna. A small distance between the metal layers of the nanoantenna provides a strong subwavelength confinement of the optical energy, enhancing light-matter interaction and overcoming the diffraction limit typical of dielectric cavities [11].
We chose a bowtie nanoantenna [22], because it affords a better localization of the optical energy inside the gap, with a weaker field confinement at the external edges compared to a typical dipole with rectangular metal strips [13]. The bowtie has dimensions of length a = 220 nm, b = 30 nm and c = 50 nm along x-axis, y-axis and z-axis, respectively. The gap between the bowtie and the PhC is denoted with G, and the distance between the metal tips with s.
The design includes a layer of flowable oxide (FOx) that covers the whole PhC cavity, as shown in Fig. 1. The FOx layer simplifies the device fabrication compared to previous designs [2], particularly reducing the manufacturing constraints for the alignment of the nanoantenna above the central holes.
The cavity provides a Q-factor of several thousand, which, combined with the very small mode volume of order $V \sim 10^{-4}\ (\lambda/n)^3$ yields an improvement of the state-of-the-art of the value of Q/V for hybrid cavities up to a value of $10^7\ (\lambda/n)^{-3}$.

3. Design of the hybrid cavity

Apart from a high Q/V factor, trapping applications demand a high transmission from the cavity, in order to achieve a high energy density in the cavity. Therefore, the 1D PhC dielectric cavity is designed to have a resonance transmission of T > 90%. We chose a nanobeam with width 490 nm and thickness 220 nm [23], hole radius R = 130 nm and period a = 320 nm to obtain a photonic bandgap in the λ = 1300 nm regime. This wavelength was chosen to reduce the water absorption with respect to λ = 1550 nm. The cavity performance is evaluated using 3D Finite Element Method (FEM) simulations, assuming a TE-polarized beam launched into the nanowire. We have taken into account the Sellmeier model to define the dispersion properties of Si and SiO_2 [24], as well as the absorption properties of water (i.e. $k = 1.2\text{x}10^{-4}$ at λ = 1380 nm) [25].
A value R_1 = 70 nm is used as the radius for the smallest hole, because larger values provide an improvement of the Q-factor, but at the expense of a decrease of the resonance transmission, so R_1 = 70 nm and Λ_1 = 260 nm are the best compromise to achieve high resonance transmission (T > 90%) and a remarkable Q-factor ($Q > 10^4$). The number of the tapered and mirror holes, N_t and N respectively, strongly influence the cavity performance. A detailed parametric analysis was carried out on both parameters; the values N_t = 6 and N = 4 returned the best compromise between a high Q-factor and high resonance transmission, obtaining $Q = 1.1\text{x}10^4$, $V = 0.5\ (\lambda/n)^3$, corresponding to $Q/V = 2.2\text{ x}10^4\ (\lambda/n)^{-3}$ and T = 93% at λ_R = 1378.8 nm. A strong energy confinement between the central holes was verified, confirming the suitability of the PhC cavity to be vertically coupled to the bowtie nanoantenna.

A parametric analysis was also carried out on the metal slot *s* and the gap layer *G* between the PhC and the bowtie to evaluate the hybrid cavity performance, as shown in Fig. 2. The Lorentz-Drude model was taken into account to simulate the Au dispersion (i.e. ε_{Au} = -76.376+8.5489i at λ = 1380 nm) [26].

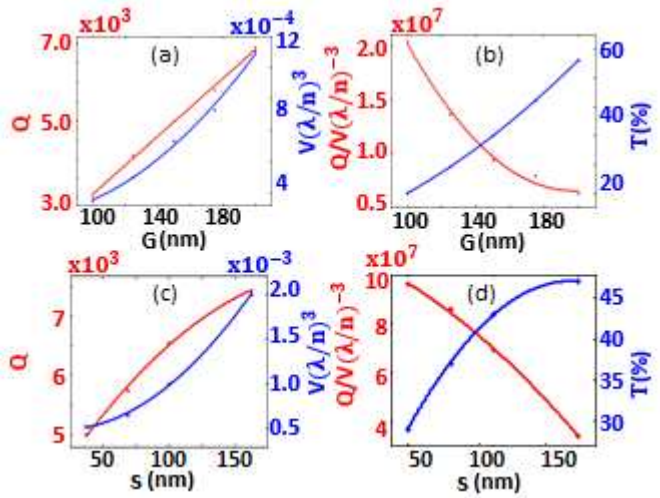

Fig. 2 Hybrid cavity performance as a function of both parameters *G* and s with a bowtie width *s* = 50 nm (a,b) and *G* = 150 nm (c,d).

As the gap layer G is increased, both the Q-factor and the resonance transmission go up, due to the reduced overlap of the mode with the metal layer and the corresponding decrease of the metal absorption, but at the expense of lower energy confinement within the bowtie. A similar behavior is observed for increasing the bowtie separation *s*, and there is an obvious increase of the mode volume for high values of *s*. Therefore, the values of *G* = 150 nm and *s* = 50 nm are taken as the best compromise between Q/V and T, obtaining $Q = 5x10^3$ and $V = 5.1x10^{-4}$ $(\lambda/n)^3$, which correspond to $Q/V = 10^7$ $(\lambda/n)^{-3}$ and T = 29% at λ = 1381.1 nm, as shown in Fig. 3(a). This performance represents an improvement over the state-of-the-art of hybrid cavities by two orders of magnitude [19], thereby providing a Q/V comparable with the values obtained by dielectric cavities [27], but with a much stronger energy confinement in very small volumes.
Fig. 3(b) illustrates the strong energy confinement in the hotspot highlighting the suitability of the hybrid cavity as a nanotweezer, particularly to trap nanoparticles with a diameter smaller than the bowtie width separation *s*.

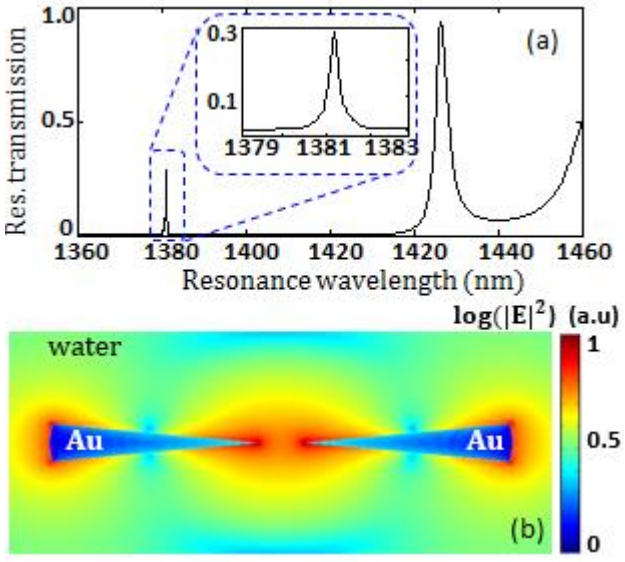

Fig. 3. (a) Transmission spectrum and (b) energy confinement at resonance in the bowtie nanoantenna of the photonic/plasmonic cavity.

4. Design of the optical nanotweezer

Next, we assess the trapping performance and calculate the optical force exerted by the cavity according to Eq. 1:

$$\mathbf{F} = \oint_S (\mathbf{T_M} \times \mathbf{n})\, dS \tag{1}$$

where $\mathbf{T_M}$ is the Maxwell stress tensor, S is the particle surface, and **n** is the vector normal to the surface [28]. For a particle with a diameter smaller than 100 nm, the optical force can be also expressed as the force gradient for a Rayleigh particle [9]:

$$F_{grad} = (n_m^2 r^3/2)[(m^2-1)/(m^2+2)]\nabla|E|^2 \tag{2}$$

where n_m is the refractive index of the medium, m is the ratio of the particle refractive index to the refractive index of the medium, and E is the electric field. The trapping of small nanoparticles is very difficult, as demonstrated by Eq. 2, because the trapping force scales as the 3rd power of radius, due to Brownian motion.

We compute the force by integrating $\mathbf{T_M}$ over a surface that has a radius 5 nm larger than the particle. An accurate evaluation of optical forces is provided by locating the boundary layers of the computational domain sufficiently far away from the particle and other scattering objects, thereby avoiding any undesired reflections of the fields at the boundary of the computational domain that could affect the evaluation of optical forces. A spherical polystyrene bead with n = 1.57, which corresponds to $m = n_{pol}/n_{H20} = 1.2$, is assumed to flow around the hybrid cavity with low speed (< 10 μm/s) to obtain a laminar flow condition. We assume a low input power (P_{in} = 1 mW) in order to minimise any thermal heating effects. The values of the optical forces along y-axis and z-axis are shown in Fig. 4, assuming y = 0 and z = 0 as the particle position when the particle is exactly centered in the middle of the bowtie nanoantenna.

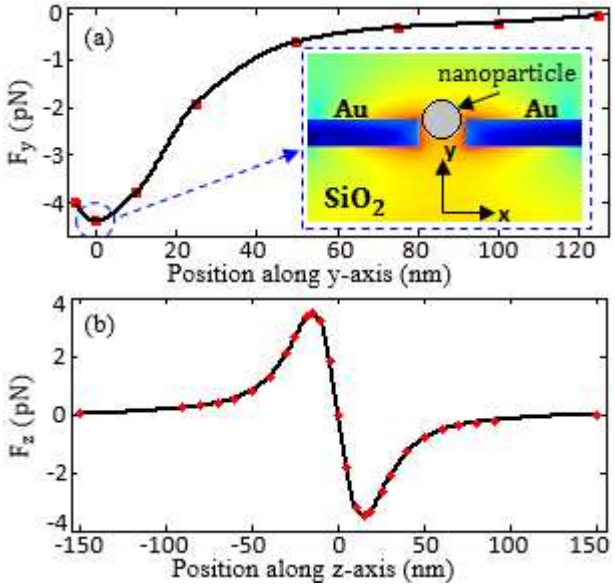

Fig. 4. Optical force for different particle positions along the y-axis with the mode distribution in the inset (a) and along z-axis (b) for a polystyrene particle with D = 40 nm and P_{in} = 1 mW.

A maximum value of the optical force of F = -4.4 pN is found at y = 0, when the particle is trapped inside the bowtie. A value of $F_y = 0$ is obtained at y = 120 nm, at which point the particle no longer experiences any trapping forces. The maximum value of the optical force along the z-axis is $F_z = \pm 3.8$ pN at ± 20 nm, while $F_z = 0$ is calculated for z = 0, which corresponds to the equilibrium point. These observations confirm that the particle flowing close to the bowtie is affected by an attractive force that carries it towards the equilibrium point, where the particle's position is kept fixed. We neglect other forces such as thermal and drag forces, because of the low input power (1 mW) and the slow laminar flow (<10 μm/s).

Next, we calculate two important figures of merit for the trapping performance: stability and stiffness. The trap stiffness is defined as [29]:

$$K = \frac{\partial F}{\partial X}\Big|_{equilibrium} \tag{3}$$

where F is the optical force, and ∂X is the particle displacement. For high values of the optical stiffness, only negligible fluctuations of the trapped particle around the equilibrium point are expected. A trapping stiffness of K = 90 pN/nm·W is obtained, about one order of magnitude higher than typical PhC dielectric cavities [29] and also higher than simple nanoantennas [28] for trapped particles of 40 nm. The stability S then describes the ratio between trapping energy and thermal energy and it quantifies the ability of the trap to hold the particle for a long time. The stability is defined as:

$$S = \frac{U}{K_B T} \tag{3}$$

where U is the work necessary to carry the particle from a free position to the equilibrium point, k_B is Boltzmann's constant, and T the ambient temperature of 300 K, which does not increase at the low input powers used here. A value of S > 10 is typically assumed as a condition for stable trapping [17] and the value we calculated for our hybrid cavity by assuming P_{in} = 1mW and a particle size of 40 nm is S = 30. We have also verified that a stable trapping condition (S > 10) can be achieved within typical manufacturing limitations, such as rounded corners of the bowtie tips with a radius up to 10 nm or a slight misalignment between the nanoantenna and the PhC with a shift of the bowtie up to ± 150 nm and ± 70 nm along x-axis and z-axis, respectively.
Fig. 5 illustrates the attractive force for a 40 nm polystyrene nanoparticle flowing near the bowtie.

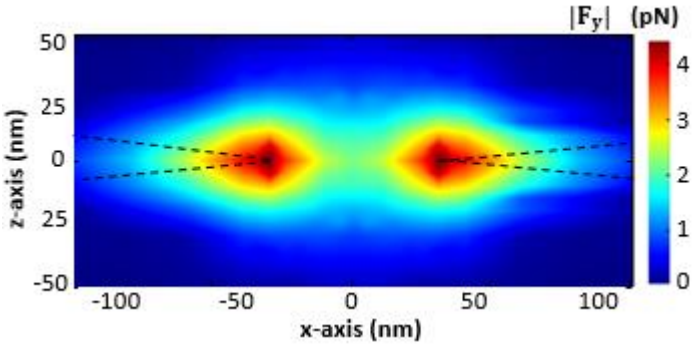

Fig. 5. Attractive force F_y on a polystyrene nanoparticle with a diameter of 40 nm and an input power P_{in} = 1 mw. The particle is placed 5 nm above the bowtie surface.

In Fig. 5, the position of the nanoparticle is assumed to be 5 nm above the surface of the bowtie and each set of values along the x-axis and the z-axis corresponds to the position of the lowest point of the particle. The maximum values of the optical force are obtained around the bowtie hotspot, as expected. The nanoparticle is affected by attractive forces in a region of about ± 50 nm along the z-axis and ± 100 nm along the x-axis, as shown in Fig. 5.
The influence of the particle diameter *D* on the nanotweezer performance is shown in figure 6.

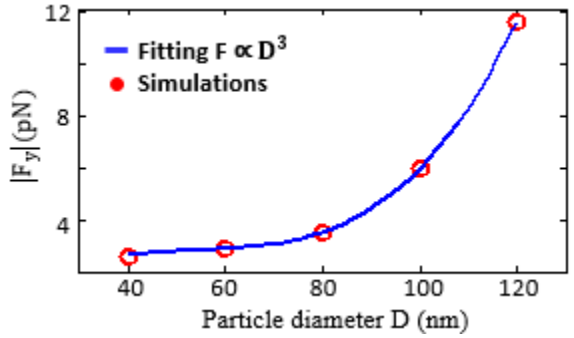

Fig. 6. Optical forces $|F_y|$ as a function of polystyrene particle size with an input power of 1mW.

As expected by Eq. 2, the optical force increases quickly when increasing the nanoparticle diameter. This calculation assumes that the particle is at the equilibrium point, which corresponds to the center of the bowtie. A maximum value for $|F_y|$ of about 12 pN is obtained for a diameter of the polystyrene particle of D = 120 nm. A corresponding increase of the stability is also verified, as expected.
A further enhancement of the nanotweezer efficiency can be obtained by improving the specific bowtie pattern, namely by arranging the nanoantenna in a quadrupole configuration. Two different versions of this arrangement are illustrated in figure 7.

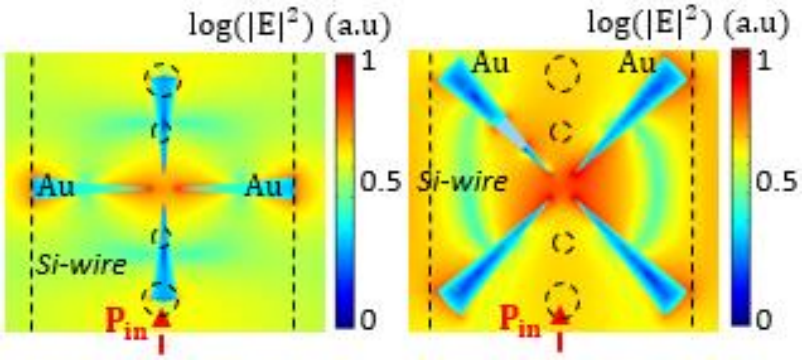

Fig.7. Mode distribution in the hybrid cavity at resonance with a quadrupole configuration (a) orthogonal and (b) tilted at 45°.

The quadrupole of Fig. 7a obtains an improvement of about 20% of the Q/V (= 1.2×10^7 $(\lambda/n)^{-3}$) compared to the simple bowtie. It also achieves stronger optical forces, up to F = -9.2 pN, even though the transmission drops slightly from T = 29% to T = 20% By rotating the quadrupole by 45°, however, we obtain a similar optical force, but bring the transmission back up to 32%, because the metal absorption is reduced when the metal strips do not overlap with the direction of light propagation in the PhC. The higher force results in a higher stability value, which in turn allows us to further decrease the input power required for stable trapping.

Conclusions

We have designed and numerically demonstrated a high performance optical tweezer for nanoparticle trapping. The hybrid cavity, comprising a 1D PhC cavity vertically coupled to a bowtie nanoantenna, has been simulated by 3D FEM simulations. We obtain a very-high Q/V ratio of 10^7 $(\lambda/n)^{-3}$ indicating a strong enhancement of the light-matter interaction. High values of optical forces of up to F = - 4.4pN on a 40 nm diameter polystyrene particle have been calculated for an input power P_{in} = 1mW. A stability, defined as the ratio between trapping energy and thermal energy, of S = 30, together with an optical stiffness of K = 90 pN/nm·W have been obtained, which confirm the excellent ability of the nanotweezer to hold particles for a long time. A further enhancement of the optical forces of up to F_{max} = - 9.2 pN has been obtained by optimizing the pattern of the nanoantenna in a quadrupole configuration, without worsening the detection resolution. This performance makes the cavity suitable for nanoparticle trapping in medical applications, such as the manipulation of small viruses, bacteria and proteins.

References

[1] K. C. Neuman, S. M. Block, Rev. Sci. Instrum. 75, 9 (2004).

[2] C. Ciminelli, D. Conteduca, F. Dell'Olio, M. N. Armenise, IEEE Phot. Journ., 6, 6, 0600916 (2014).

[3] D. Erickson, X. Serey, Y. F. Chen, S. Mandal, Lab on Chip, 11, 6 (2011).

[4] M. Dienerowitz, M. Mazilu, K. Dholakia, Journ. of Nanophotonics, 2, 021875, (2008).

[5] R. De La Rue, H. Chong, M. Gnan, N. Johnson, I. Ntakis, P. Pottier, M.Sorel, Ahmad Md Zain, Hua Zhang, E. Camargo, C. Jin, M. Armenise, C. Ciminelli, New Journ. of Phys., 8, 256 (2006).

[6] S. Lin, E. Schonbrun, K.Crozier, Nano Lett., 10, 7 (2010).

[7] S. Lin, K. Crozier, ACS Nano, 7, 2 (2013).

[8] T. van Leest, J. Caro, Lab on a chip, 13, 22 (2013).

[9] Y. F. Chen, X. Serey, R. Sarkar, P. Chen, D. Erickson, Nano Lett., 12, 3 (2012).

[10] C. Ciminelli, F. Dell'Olio, D. Conteduca, T. F. Krauss, M. N. Armenise, 16th ICTON, Graz, Austria (2014).

[11] A. Z. Oskuie, H. Jiang, B.R. Cyr, D. W. Rennehan, A. A. Al-Balushi, R. Gordon, 13, 13 (2013).

[12] C.Y.A. Ni, S.-Wei Chang, S. L. Chuang, P. J. Schuck, Jour. Of Lightw. Tech., 29, 20 (2011).

[13] W. Zhang, L. Huang , C. Santschi, O. J. F. Martin, Nano Lett., 10, 3 (2010).

[14] K. Wang, E. Schonbrun, P. Steinvurzel, K. B. Crozier, Nat. Comm, 2, 1 (2011).

[15] Y. Pang, R. Gordon, Nano Lett., 12, 1 (2012).

[16] B. J. Roxworthy, K. D. Ko, A. Kumar, K. H. Fung, E. K. C. Chow, G. L. Liu, N. X. Fang, K. C. Toussaint Jr, Nano Lett, 12, 2 (2012).

[17] X. Serey, S. Mandal, Y. F. Chen, D. Erickson, Phys. Rew. Lett., 108, 4, 048102 (2012).

[18] M. K. Kim, S. H. Lee, M. Choi, B. H. Ahn, N. Park, Y.-H Lee, B. Min, Opt. Exp., 18, 11 (2010).

[19] X. Yang, A. Ishikawa, X. Yin, X. Zhang, ACS Nano, 5, 4 (2011).
[20] M.A. Santiago-Cordoba, M. Cetinkaya, S.V. Boriskina, F. Vollmer, M.C. Demirel, J. Biophotonics 5, 8 (2012)
[21] Q. Quan, M. Loncar, Opt. Exp., 19, 19 (2011).
[22] W. Ding, R. Bachelot, S. Kostcheev, P. Royer, R. E. De Lamaestre, J. Appl. Phys., 108, 12, 124314 (2010).
[23] D. Conteduca, F. Dell'Olio, C. Ciminelli, T. F. Krauss, M. N. Armenise, 3rd MEPHOCO, Trani, Italy (2014).
[24] I. H. Malitson, J. Opt. Soc. Amer., 55, 10 (1965).
[25] K. F. Palmer, D. Williams, J. Opt. Soc. Amer., 64, 8 (1974).
[26] A. D. Rakic, A. B. Djurisic, J. M. Elazar, M. L. Majewski, Appl. Opt., 37, 22, (1998).
[27] H. Sekoguchi, Y. Takahashi, T. Asano, S. Noda, Opt. Expr., 22, 1 (2014).
[28] M. Ploshner, M. Mazilu, T. F. Krauss, K. Dholakia, J. Nanophoton., 4, 1, 041570 (2010).
[29] X Serey, S Mandal, D Erickson, Nanotechnology, 21, 30, 305202 (2010).